Trajectory Optimization for Missions to Small Bodies with a Focus on Scientific Merit

Jacob A. Englander*, Matthew A. Vavrina†, Lucy F. Lim*, Lucy A. McFadden*, Alyssa R. Rhoden‡, Keith S. Noll*
*NASA Goddard Space Flight Center
†a.i. solutions, Inc.
‡Arizona State University

***Abstract*—Trajectory design for missions to small bodies is tightly coupled both with the selection of targets for a mission and with the choice of spacecraft power, propulsion, and other hardware. Traditional methods of trajectory optimization have focused on finding the optimal trajectory for an *a priori* selection of destinations and spacecraft parameters. Recent research has expanded the field of trajectory optimization to multidisciplinary systems optimization that includes spacecraft parameters. The logical next step is to extend the optimization process to include target selection based not only on engineering figures of merit but also scientific value. This paper presents a new technique to solve the multidisciplinary mission optimization problem for small-bodies missions, including classical trajectory design, the choice of spacecraft power and propulsion systems, and also the scientific value of the targets. This technique, when combined with modern parallel computers, enables a holistic view of the small body mission design process that previously required iteration among several different design processes.**

I. Introduction

Preliminary design of interplanetary missions is a complex problem which is very expensive in terms of both human-hours and computer-hours. In any interplanetary mission design, the designer must select the appropriate launch date, flight time, maneuvers, and in some cases a sequence of planetary flybys. The choice of launch vehicle is also partly driven by trajectory design. If the mission employs low-thrust electric propulsion, then the trajectory design also includes a time history of control variables, such as thrust magnitude and direction, and is tightly coupled with the choice of propulsion and power systems for the spacecraft.

Missions to small solar system bodies are especially challenging because in addition to all of the common design tasks listed above, it is also necessary to choose one or more small bodies to visit. This process is particularly difficult because the most scientifically desirable targets may not be the most reachable and vice versa. In addition, many compelling small body mission concepts involve visiting several bodies, and the most compelling bodies may or may not be on similar orbits. The preliminary design process for such missions often involves many iterations between planetary scientists, trajectory analysts, and systems engineers until a target set, spacecraft, and trajectory are found that are satisfactory. This process is time consuming and expensive and therefore any automation that could reduce the cost and increase the quality of the mission concept is highly desirable. Furthermore, each trajectory must be evaluated according to both science and engineering metrics. The full small bodies mission optimization problem is therefore multi-objective and includes both discrete and continuous variables that define the science targets, the spacecraft, and the trajectory.

The history of interplanetary trajectory optimization is long and includes contributions by thousands of authors. A complete survey of the many interesting and useful techniques is impossible in the context of this paper. Many of the most successful techniques have been incorporated into common early-stage mission design tools [1], [2], [3], [4]. However, most of the research on the interplanetary trajectory optimization problem has focused on finding the optimal trajectory for an *a priori* chosen sequence of destinations and set of spacecraft parameters. This is only one piece of the small body mission design puzzle.

Recent research has employed evolutionary optimization techniques to solve the problem of choosing not only the optimal trajectory for a given set of destinations, but also the choice of intermediate planetary flybys which may increase the delivered mass to the final science targets for missions employing either high-thrust chemical propulsion [5], [6], [1] or low-thrust electric propulsion [7], [2], [8]. Other recent works have addressed multi-objective optimization of both the trajectory and the spacecraft design, which are tightly coupled [9]. Some works have even considered the choice of science targets [8], [10], [2], and the second through seventh editions of the Global Trajectory Optimization Contest (GTOC) [11] have featured the problem of choosing targets for missions which visit many small bodies. In particular, the sixth edition of GTOC was a tour of the Galilean moons of Jupiter and featured an objective function that rewarded trajectories which flew over as many faces of each body as possible.

However, all of these works have focused on choosing trajectories and destinations based on engineering metrics, *e.g.* Δv, delivered mass, flight time, *etc.*. To the knowledge of these authors, no previous integrated scheme has solved the full coupled problem - the choice of destination, spacecraft parameters, and trajectory in a multi-objective fashion such that one of the explicit objectives of the solver is to find the most scientifically compelling missions.

In this work we present a method which solves the full coupled problem for small body mission design. The design problem is posed as a multi-objective hybrid optimal control

problem (HOCP) with two stages, an "outer-loop" which chooses candidate values for the discrete parameters such as destinations, intermediate flybys, and spacecraft systems options, and an "inner-loop" which finds the optimal trajectory for each candidate set of discrete parameters. The outer-loop ranks the candidate missions by several objectives including both engineering figures of merit such as delivered mass and flight time and also a scoring system for scientific value.

II. Physical Modeling

A. Mission Architecture

Three trajectory components or trajectory divisions are defined in this work: *missions*, *journeys*, and *phases*. A *mission* is a top-level container that encompasses all of the events including departures, arrivals, thrust arcs, coast arcs, and flybys. A *journey* is a set of events within a mission that begin and end at a target of interest. In the context of this work, a *journey* begins at either the Earth or a small body and ends at another small body. Each journey may include any number of planetary flybys, which split the journey into *phases*. For example, NASA's OSIRIS-REx mission is composed of two journeys - from the Earth to Bennu and from Bennu back to the Earth. The outbound journey includes an Earth gravity assist and therefore has two phases, and the return journey has no gravity assists and therefore consists of a single phase.

B. Modeling of Dynamics

The dynamics of the spacecraft motion are modeled using the Sims-Flanagan transcription (SFT), a widely-used method in which the continuous-thrust trajectory is discretized into many small time steps, and the thrust applied during each time step is approximated as a small impulse placed at the center of the time step [12]. While the number of SFT time steps necessary to approximate the trajectory with reasonable accuracy is problem dependent, 10-20 time steps per orbit about the central body is usually sufficient The SFT, when used with a nonlinear programming (NLP) problem solver such as the Sparse Nonlinear Optimizer (SNOPT)[13] and a suitable initial guess, is very fast and robust. It is considered to be a "medium-fidelity" transcription and is used in several industry-standard software packages [2], [3], [4].

In the classical SFT, the optimizer chooses the three components of an impulsive $\Delta\mathbf{v}$ vector at the center of each time-step. In order to improve the robustness of the solver, a modified transcription known as "up-to-unit vector control" [14] is used in this work, where instead of choosing the $\Delta\mathbf{v}$ vector directly the optimizer instead chooses a control 3-vector in $[-1.0, 1.0]$ that is multiplied by the maximum Δv that the spacecraft can produce in that time-step. The magnitude of the control vector is bounded in the range $[0.0, 1.0]$, i.e.,

$$\Delta\mathbf{v}_i = \mathbf{u}_i \Delta v_{max,i}, \|\mathbf{u}_i\| \leq 1.0 \tag{1}$$

where

$$\Delta v_{max,i} = \frac{D n_{available} T \left(t_f - t_0\right)}{mN} \tag{2}$$

where D is the thruster duty cycle, $n_{available}$ is the number of available thrusters, T is the maximum available thrust from one thruster, t_0 and t_f are the beginning and ending times of the time step, m is the mass of the spacecraft at the center of the time step, and N is the number of time steps in the phase. This modified SFT is used in Mission Analysis Low-Thrust Optimization (MALTO), Parallel Global Multiobjective Optimizer (PaGMO), and in this work.

The spacecraft state is propagated forward from the first endpoint (*i.e.* planet) in each phase and backward from the second endpoint. The trajectory is propagated by solving Kepler's equation and the spacecraft mass is propagated by assuming a constant mass flow rate across the each time-step. A set of nonlinear constraints are applied to ensure continuity of position, velocity, and mass in the center of the phase.

The optimizer also chooses the initial and final velocity vectors for each phase. If a phase begins with a launch, the magnitude of the initial velocity vector is used with a launch vehicle model to determine the initial mass of the spacecraft as described later in this work. If a phase begins with a planetary flyby, two nonlinear constraints are applied to ensure that the flyby is feasible. First, the magnitudes of the incoming and outgoing velocity vectors with respect to the planet must be equal,

$$v_\infty^+ - v_\infty^- = 0 \tag{3}$$

where v_∞^- and v_∞^+ are the magnitudes of the velocities before and after the flyby, respectively. Second, the spacecraft may not fly closer to the planet than some user-specified minimum flyby distance:

$$\frac{\mu_{planet}}{v_\infty^2}\left[\frac{1}{\sin(\frac{\delta}{2})} - 1\right] - (r_{planet} + h_{safe}) \geq 0 \tag{4}$$

where

$$\delta = \arccos\left[\frac{\mathbf{v}_\infty^- \cdot \mathbf{v}_\infty^+}{|v_\infty^-|\,|v_\infty^+|}\right] \tag{5}$$

Here μ_{planet} is the gravitational parameter of the planet, r_{planet} is the radius of the planet, δ is the flyby turn angle, and h_{safe} is the user-defined minimum altitude. In the case of a flyby of a small body without significant gravitational influence, Equations 3-5 are replaced by:

$$\mathbf{v}_\infty^+ - \mathbf{v}_\infty^- = \mathbf{0} \tag{6}$$

Figure 1 is a diagram of a simple low-thrust mission to Jupiter with one Earth flyby using the SFT. Here the Earth flyby occurs approximately one year after launch. The continuity constraints are deliberately left unsatisfied in the diagram to illustrate where they must be applied.

The SFT is a compromise between medium-fidelity modeling and fast execution. It is ideal for a trade study optimization such as the problem considered in this work, and solutions found using the SFT are an excellent starting point for more detailed analysis once a reference mission is chosen. Typically the mass delivered by a SFT trajectory is within 1-2% of a that delivered by a higher-fidelity solution [15].

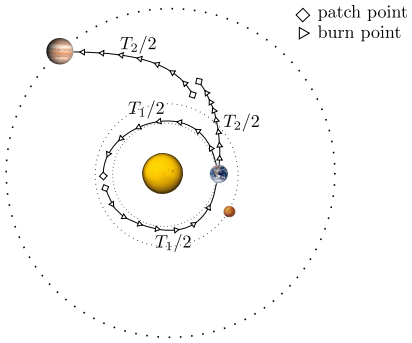

Fig. 1: Schematic of a two-phase trajectory using the SFT

C. Launch Vehicle, Propulsion, Power, and Ephemeris Modeling

Low-thrust trajectories are inextricably coupled to the specific hardware used by the spacecraft. The optimal trajectory for one combination of launch vehicle, propulsion system, and power system will not be the optimal trajectory for a different hardware combination. Realistic modeling of these three systems and of system margins is therefore applied in this work. In addition, accurate ephemeris modeling is provided by the SPICE toolkit [16].

Launch vehicle performance, measured as delivered mass in kg as a function of C_3 in km^2/s^2, is modeled as a 5^{th} degree polynomial with coefficients fit to published launch vehicle performance data[17]. In this work, a simplified thruster model is applied to compute available thrust T as a function of available power, fixed propulsion system efficiency η and specific impulse (I_{sp}),

$$T = \frac{2\eta P}{I_{sp} g_0} \tag{7}$$

where I_{sp} and η are defined based on thruster performance. This is one of several models that may be used for low-thrust mission designs. Other, more detailed models, are available to interested readers [2].

The available power P is the difference between the power generated by the spacecraft $P_{generated}$ and the power required to operate the spacecraft bus $P_{s/c}$,

$$P = (1 - \delta_{power}) \left(P_{generated} - P_{s/c} \right) \tag{8}$$

where δ_{power} is a user-defined power margin.

In this work, the power delivered by a radioisotope thermoelectric generator (RTG) system is given by,

$$P(t) = P_0 e^{(-t/\tau)} \tag{9}$$

where P_0 is the base power delivered by the RTG on the day of launch and τ is the decay rate of RTG. The power required by the spacecraft bus $P_{s/c}$ is modeled as a constant in this work. More sophisticated power models suitable for solar-electric propulsion (SEP) missions are available but are omitted from this work in the interest of brevity [2].

III. Outer-Loop Optimization of the Mission Sequence

The mission design problem in this work is posed as two nested optimization problems, an "outer-loop" discrete optimization problem and an "inner-loop" real-valued optimization problem. The outer-loop solves for the sequence variables such as destinations and flybys, driving temporal variables such as date and flight time, as well as system parameters such as power supply size, propulsion system, and launch vehicle. A "cap and optimize" process is applied to certain outer-loop parameters such as flight time, allowing the inner loop to vary those parameters within a maximum or minimum value.

The user specifies *a priori* a list of outer-loop design variables and a "menu" of choices with corresponding integer codes for each. In this work the design variables are spacecraft systems parameters such as power and/or propulsion, time of flight, destinations, and planetary flybys that may occur between small body destinations. The outer-loop algorithm makes one choice from each menu.

In this work the outer-loop's ability to select destinations is particularly relevant. The user specifies a menu of candidate destinations for each journey. For example, one might wish to design a mission to two asteroids but have a long list of scientifically interesting options. The HOCP automaton can choose the most accessible asteroids. The outer-loop can also control the number of destinations, and therefore the number of journeys, by using a "null-gene" technique [1]. In this technique, the menu of journey destinations is augmented to include a number of "null" options equal to the number of acceptable bodies. The outer-loop therefore has an equal probability of selecting "no encounter" as it does of selecting an encounter. The same technique is used to select the number and identity of any planetary flybys that might occur in each journey. This technique is effective for designing multi-flyby interplanetary missions and has been used to reproduce the Cassini [1] trajectory and design an efficient variant of the BepiColombo trajectory [2].

The user may then select any number of outer-loop objective functions for optimization. Some of these, such as flight time, power system size, *etc*, may be directly related to decision variables. Others, such as final mass, may be results of an inner-loop optimization. In the particular context of this work, the list of objective functions include a science score which is a function of the destinations chosen by the outer-loop.

The outer-loop constructs an inner-loop subproblem which is capped according to the information encoded in the outer-loop decision vector. The inner-loop subproblem is then optimized with respect to a single objective function as chosen by the user. Finally, the values of the outer-loop objective functions are extracted from the completed inner-loop solution.

A. Outer-Loop Multi-Objective Optimization via NSGA-II

The goal of the outer-loop, multi-objective algorithm is to generate a representation of the globally-optimal Pareto front [18]. The interplanetary, low-thrust trajectory design problem is almost always a compromise between maximizing payload mass and minimizing time of flight. When simultaneously

solving the systems problem, other objectives such as reducing the base power required for thrusting and minimizing the number of low-thrust engines become important. Thus, the globally-optimal Pareto front represents the critical set of system trade-off solutions desired. However, the system design parameters are often discrete hardware models and an algorithm that is capable of automated development of the Pareto front while globally searching the design space is required. One such algorithm that meets the required characteristics of an outer-loop systems optimizer is the Non-Dominated Sorting Genetic Algorithm II (NSGA-II) developed by Deb *et al.* [19]. Non-Dominated Sorting Genetic Algorithm II (NSGA-II) has ben shown to be an effective outer-loop solver for multi-objective, low-thrust optimization in a global-local hybrid strategy [8], [9]. The NSGA-II is a modification of the simple genetic algorithm [20], and instead of evolving the population towards a single solution, genetic operators (selection, crossover, mutation) steer the population towards the Pareto front.

The NSGA-II is notably efficient because of the employment of elitism, in which the superior solutions of the population are retained from generation to generation. By performing a non-dominated ranking of a combined parent-and-offspring population and filtering for the best solutions, the NSGA-II can ensure that the individuals that are closest to the Pareto front are not lost as the population evolves. Additionally, the NSGA-II incorporates mechanisms to improve population diversity by ranking individuals in a particular non-dominated front according to their crowding distance in the solution space. The particular implementation of NSGA-II used in this work was developed by Vavrina *et al.* [8], [9] and provides improved performance over the original NSGA-II on problems with more than two objective functions. This is a very useful feature in this work, where the example problem has five objectives.

IV. Inner-Loop Trajectory Optimization

In order for the outer-loop solver of an HOCP automaton to function properly, it must know the values of the objective functions for each candidate solution. Finding these values is the job of the inner-loop solver. The inner-loop solver must be fast and autonomous, because in the context of an automated HOCP solver there is no opportunity for a human to intervene to provide an initial guess of the solution. In this work, the inner-loop solver is a combination of a NLP problem solver with the stochastic global search algorithm monotonic basin hopping (MBH).

A. Nonlinear Programming

The optimization of the multiple gravity assist with low-thrust (MGALT) problem may be formulated as nonlinear programming (NLP) problems. NLP problems explicitly model nonlinear constraints. The optimizer solves a problem of the form:

$$\begin{aligned} &\text{Minimize } f(\mathbf{x}) \\ &\text{Subject to:} \\ &\mathbf{x}_{lb} \leq \mathbf{x} \leq \mathbf{x}_{ub} \\ &\mathbf{c}(\mathbf{x}) \leq \mathbf{0} \\ &A\mathbf{x} \leq \mathbf{0} \end{aligned} \tag{10}$$

where $\mathbf{x}_{lb}$ and $\mathbf{x}_{ub}$ are the lower and upper bounds on the decision vector, $c(\mathbf{x})$ is a vector of nonlinear constraint functions, and A is a matrix describing any linear constraints (*i.e.* time constraints).

Almost all low-thrust interplanetary trajectory optimization problems, are very large, composed of hundreds or thousands of decision variables and tens or hundreds of constraints. A large-scale NLP solver such as SNOPT [13] is therefore required to solve the problems of interest in an efficient and robust manner. However, SNOPT, like all NLP solvers, requires an initial guess of the solution and will tend to converge to a solution in the neighborhood of that initial guess. The next section will address how the automated method of this work generates this initial guess in a fully automated manner.

B. Monotonic Basin Hopping

MBH is an algorithm for finding globally optimal solutions to problems with many local optima. MBH works on the principle that many real-world problems have a structure where individual local optima, or "basins" tend to cluster together into "funnels" where one local optimum is better than the rest. A problem may have several such funnels. MBH has been demonstrated to be effective on various types of interplanetary trajectory problems [21], [22], [23], [24], [2]. The pseudocode for MBH is listed in Algorithm 1.

V. Example

The algorithm described in this work is demonstrated on a notional mission to survey the Centaurs. The Centaurs are a class of minor planets that orbit, approximately, between Saturn and Neptune. The Centaurs are not in resonance with the gas giants and are therefore on unstable orbits that will cause them to eventually be pushed into the inner solar system, collide with a gas giant, or ejected entirely. They may originally have been Kuiper Belt Object (KBO)s that were perturbed closer to the inner solar system and may be on their way to becoming comets. Some Centaurs have shown comet-like characteristics such as displaying a coma near perihelion. For the purposes of this example, the Centaurs are of particular interest because they are more accessible for rendezvous than the KBOs and may provide a window into the early solar system using near-term propulsion and power technology.

The Centaurs have bimodal colors: red and blue/gray [25], [26]. The ideal mission to survey the Centaurs would visit one of each class. In addition, for the purposes of this example there are three Centaurs of particular interest: 2060 Chiron, 10199 Chariklo, and 60558 Echeclus. Chiron displays a coma near perihelion and may have rings [27], Chariklo has rings [28], and Echeclus recently ejected a large amount of

Algorithm 1 Monotonic Basin Hopping (MBH)

generate random point $\mathbf{x}$
run NLP solver to find point $\mathbf{x}^*$ using initial guess $\mathbf{x}$
$\mathbf{x}_{current} = \mathbf{x}^*$
if $\mathbf{x}^*$ is a feasible point **then**
  save $\mathbf{x}^*$ to archive
end if
while not hit stop criterion **do**
  generate $\mathbf{x}'$ by randomly perturbing $\mathbf{x}_{current}$ using a Pareto distribution
  for each time of flight variable t_i in $\mathbf{x}'$ **do**
    if $rand\,(0,1) < \rho_{time-hop}$ **then**
      shift t_i forward or backward one synodic period
    end if
  end for
  run NLP solver to find locally optimal point $\mathbf{x}^*$ from $\mathbf{x}'$
  if $\mathbf{x}^*$ is feasible **and** $f\,(\mathbf{x}^*) < f\,(\mathbf{x}_{current})$ **then**
    $\mathbf{x}_{current} = \mathbf{x}^*$
    save $\mathbf{x}^*$ to archive
  else if $\mathbf{x}^*$ is infeasible **and** $\|c\,(\mathbf{x}^*)\| < \|c\,(\mathbf{x}_{current})\|)$
    $\mathbf{x}_{current} = \mathbf{x}^*$
  end if
end while
return best $\mathbf{x}^*$ in archive

material [29]. A scoring system was constructed in which 10 points are awarded for the first red Centaur, 10 for the first blue/grey Centaur, and 1 "bonus" point for Chiron, Chariklo, or Echeclus. The "bonus" point is allowed to stack with the classification points. We assume that one body of each class is sufficient, so the maximum science score for any candidate mission is 21 points for a mission that includes a red, a blue/grey, and one of the "special" Centaurs. Table I is a list of the Centaurs and describes how they are classified for this example.

We also score each candidate mission by the number of encounters. In this example the outer-loop is allowed to choose not only the number of targets and the identity of the targets, but also whether each encounter is a flyby, in which the spacecraft matches position only, or a rendezvous, in which the spacecraft matches both the position and velocity of the object. A rendezvous is considered to provide greater science value than a flyby but requires more time and propellant. Accordingly, 10 encounter points are awarded for each rendezvous and one encounter point is awarded for each flyby.

The spacecraft in this example employs a radioisotope-electric propulsion (REP), a system composed of a RTG and a small electric thruster. Such a system is ideal for a mission such as a multi-Centaur tour, which may need to perform significant maneuvers in the outer solar system where SEP is not viable and chemical propulsion cannot provide sufficient Δv to reach more than one Centaur. This approach was used for a previous study that considered a rendezvous with 2060 Chiron as part of the 2010 Planetary Science Decadal Survey [31]. In this study the propulsion system is modeled as having an I_{sp} of 1500 s and a system efficiency η of 0.485. The available thrust is then computed as a function of

TABLE I: List of classified Centaurs [30]

Name	Classification	Science score
2060 Chiron	BG, special	11
8405 Asbolus	BG	10
10199 Chariklo	BG, special	11
10370 Hylonome	BG	10
60558 Echeclus	BG, special	11
29981	BG	10
32532 Thereus	BG	10
42355 Typhon	BG	10
49036 Pelion	BG	10
52872 Okyrhoe	BG	10
54598 Bienor	BG	10
60608	BG	10
63252	BG	10
73480	BG	10
91554	BG	10
95626	BG	10
119315	BG	10
120061	BG	10
127546	BG	10
248835	BG	10
342842	BG	10
427507	BG	10
5145 Pholus	R	10
31824 Elatus	R	10
33128	R	10
44594	R	10
52975 Cyllarus	R	10
55576 Amycus	R	10
65489 Ceto	R	10
7066 Nessus	R	10
83982 Crantor	R	10
87269	R	10
121725	R	10
308933	R	10
469750	R	10

available power via equation 7. The RTG system is modeled via Equation 9, where the decay rate τ is set to 2% per year. We assume that P_0 is bought in discrete units of 425 W, with the number of units chosen by the outer-loop solver. The spacecraft is assumed to require 250 W for non-propulsion power.

In this example, the outer-loop is allowed to choose the destination Centaurs, whether each Centaur encounter is a flyby or a rendezvous, whether or not there will be planetary gravity assists and if so which ones and how many, the upper bound on the time of flight, and the number of RTG units. The inner-loop then finds the trajectory that delivers the most mass to the final Centaur encounter for each candidate outer-loop solution. The outer-loop seeks to find the five-dimensional non-dominated trade surface ranked by power system size, time of flight, and the science merit score and encounter score described above. Table II lists the assumptions and solver settings. There are 2.3×10^14 solutions to the outer-loop problem. It is impractical to evaluate all of them, and so the NSGA-II-based outer-loop in this work is necessary.

The HOCP automaton was run with an outer-loop population size of 300 for 305 generations on a 60-core Intel Xeon E7-4890 v2 server running at 2.8 GHz. This took thirteen days with no human intervention. A plot of the final population is shown in Figure 2. P_0, flight time, and mass are the x, y, and z axes of the plot. Science merit score is represented as a color, where redder is better, and encounter

TABLE II: Assumptions common to all candidate Centaur missions

Option	Value
Earliest allowable launch date	1/1/2030
Latest allowable launch date	12/31/2040
Flight time upper bound	10 to 50 years, chosen by outer-loop
Launch vehicle	Atlas V 551 with Star 48 upper stage
Number of 425 W RTGs	1 to 10
RTG decay rate	2% per year
Spacecraft bus power $P_{s/c}$	250 W
Thruster I_{sp}	1500
Thruster efficiency η	0.485
Duty cycle	90%
Power margin	15%
Propellant margin	10%
Number of time steps per phase	20
Centaurs	up to four from Table I
Gravity assists (before first Centaur)	up to 3 of Venus, Earth, Mars, and/or Jupiter
Gravity assists (between Centaurs)	up to 2 of Jupiter, Saturn, Uranus, and/or Neptune
Centaur encounter type	flyby or rendezvous
Stay time at rendezvous targets	1 year
Outer-loop NSGA-II Population Size	300
Outer-loop NSGA-II μ_{GA}	0.15
Inner-loop MBH run time	20 minutes
Inner-loop MBH Pareto α	1.3
Inner-loop MBH $\rho_{time-hop}$	0.2

Fig. 2: Final generation of the outer-loop, showing non-dominated solutions

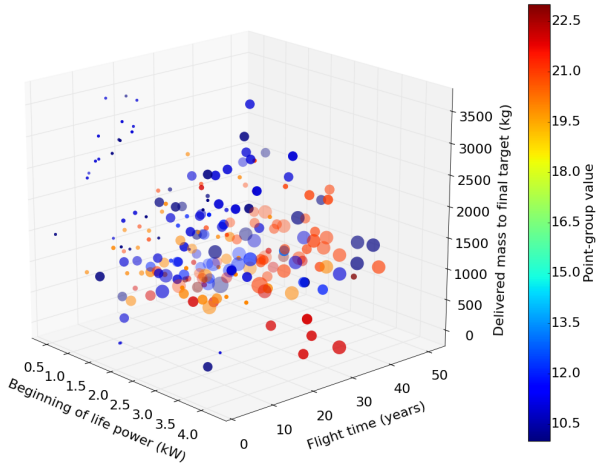

score is represented as marker size. Each marker on the plot is a separate mission, with a unique combination of objective function scores. Each mission may have a different power system, flight time, set of gravity assists, or even different Centaurs. It is difficult to visualize a 5-dimensional trade space in a 3-dimensional plot, but in the interactive version one may rotate the plot and click on individual missions to examine them in detail. This interface is designed to make it easy for a team of scientists and flight dynamicists to choose one or more candidate missions for further study. In all, the HOCP automaton explored 68963 possible solutions and thus the inner-loop was run 68963 times. Figure 2 shows only 300 non-dominated missions from that set.

In the interest of brevity, we will examine only three

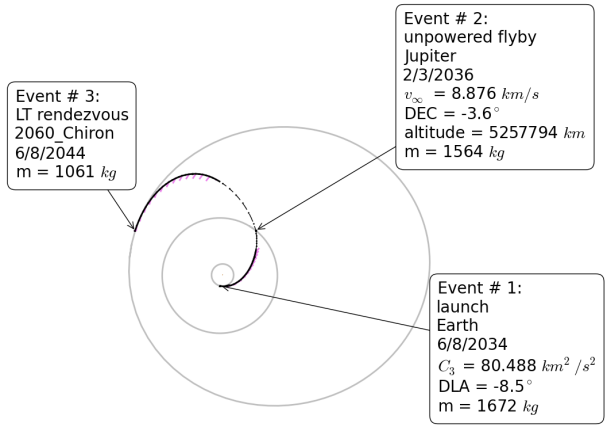

Fig. 3: A 10 year mission to Chiron (BG, special) using a 1275 W power system, 11 science points, 10 encounter points

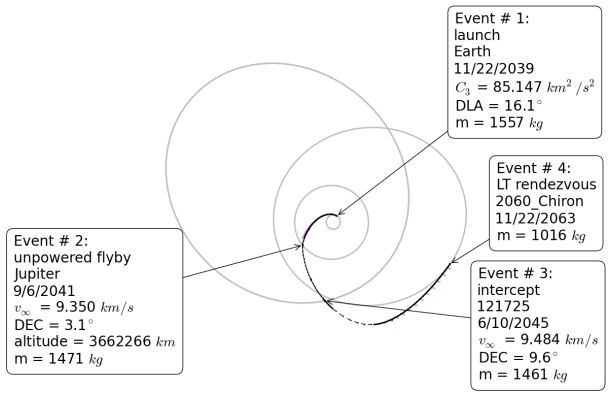

Fig. 4: A 24 year mission to fly by 121725 (R) and rendezvous with Chiron (BG, special) using an 850 W power system, 11 science points, 10 encounter points

trajectories in detail. Figure 3 describes a relatively short 10-year mission to 2060 Chiron, one of the highest science value targets. The flight time is short enough for a viable New Frontiers-class mission but since only one target is reached the goal of surveying the Centaurs is not accomplished. The power system is also quite large at 1275 W. Figure 4 shows a 24-year mission to fly by 121725 (red) and then rendezvous with 2060 Chiron (blue/grey). This mission accomplishes the objective of surveying the different classes of Centaur and reaches a high-priority target with a reasonable power system, but the flight time is quite long. Finally, Figure 5 depicts a 36-year mission to rendezvous with both 31824 Elatus (red) and 49036 Pelion (blue/grey) using a 1700 W power system. This mission is the shortest to provide detailed science opportunities at both classes of Centaur without requiring an extremely large power system, but at 1700 W the power requirement already stretches what may be reasonable for next-generation RTGs. In general, as power increases, flight time decreases and encounter score and delivered mass increase. Since encounter score is loosely coupled to science score, more power also means better science. Any of these missions, or others from Figure 2, could be selected for further analysis by a scientist and his or her team.

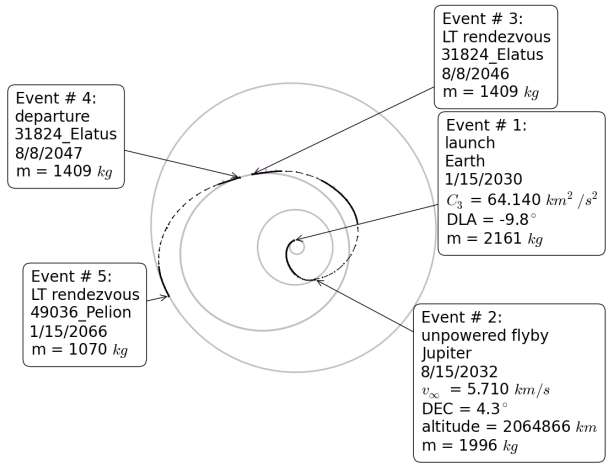

Fig. 5: A 36 year mission to rendezvous with 31824 Elatus (R) and 49036 Pelion (BG) using a 1700 W power system, 20 science points, 20 encounter points

VI. Conclusion

This work presents an HOCP automaton that is capable of mapping the multi-objective trade space between spacecraft system parameters, trajectory characteristics, and science value for a wide variety of small body missions. The algorithm is demonstrated on a hypothetical multi-Centaur tour and provides a trade-space map that a scientist could use to choose one or more candidate missions for further study. The intent of this algorithm is to simplify and speed up the beginning of the mission proposal process, in which scientists and engineers search for the right trade between science value and engineering feasibility that can be turned into a proposal. The example presented in this work is somewhat fanciful and is deliberately not tied to any current mission proposal, but illustrates the capabilities of the algorithm.

The algorithms presented in this work are implemented in the Evolutionary Mission Trajectory Generator EMTG, NASA Goddard Space Flight Center's tool for the preliminary design of planetary science missions. This tool is an integral part of Goddard's current proposal design process, and was used to support the recently selected Lucy proposal.

Acknowledgments

The authors would like to acknowledge Donald Ellison, Dr. Alexander Ghosh, and Professor Bruce Conway at the University of Illinois, Dr. Jeremy Knittel and Kyle Hughes at NASA Goddard Space Flight Center, and Dr. Bruno Sarli at the Catholica University of America for their ongoing contributions to Evolutionary Mission Trajectory Generator (EMTG). This research was a by-product of Planetary Science mission proposal efforts at NASA Goddard Space Flight Center.

References

[1] Englander, J. A., Conway, B. A., and Williams, T., "Automated Mission Planning via Evolutionary Algorithms," *Journal of Guidance, Control, and Dynamics*, Vol. 35, No. 6, 2012, pp. 1878–1887, doi: 10.2514/1.54101.

[2] Englander, J. A. and Conway, B. A., "An Automated Solution of the Low-Thrust Interplanetary Trajectory Problem," *Journal of Guidance, Control, and Dynamics*. Accepted.

[3] McConaghy, T. T., *GALLOP Version 4.5 User's Guide*, School of Aeronautics and Astronautics, Purdue University, 2005.

[4] Sims, J., Finlayson, P., Rinderle, E., Vavrina, M., and Kowalkowski, T., "Implementation of a Low-Thrust Trajectory Optimization Algorithm for Preliminary Design," in "AIAA/AAS Astrodynamics Specialist Conference and Exhibit," AIAA Paper 2006-6746, 2006, doi: 10.2514/6.2006-6746.

[5] Gad, A. and Abdelkhalik, O., "Hidden Genes Genetic Algorithm for Multi-Gravity-Assist Trajectories Optimization," *Journal of Spacecraft and Rockets*, Vol. 48, No. 4, 2011, pp. 629–641, doi: 10.2514/1.52642.

[6] Gad, O. A. A., "Dynamic-Size Multiple Populations Genetic Algorithm for Multigravity-Assist Trajectories Optimization," *Journal of Guidance, Control, and Dynamics*, Vol. 35, No. 2, 2012, pp. 520–529, doi: 10.2514/1.54330.

[7] Vasile, M. and Campagnola, S., "Design of low-thrust multi-gravity assist trajectories to Europa," *Journal of the British Interplanetary Society*, Vol. 62, No. 1, 2009, pp. 15–31.

[8] Englander, J., Vavrina, M., and Ghosh, A., "Multi-Objective Hybrid Optimal Control for Multiple-Flyby Low-Thrust Mission Design," in "AAS/AIAA Space Flight Mechanics Meeting, Williamsburg, VA," , 2015. Paper AAS 15-227.

[9] Vavrina, M., Englander, J., and Ghosh, A., "Coupled Low-Thrust Trajectory and Systems Optimization Via Multi-objective Hybrid Optimal Control," in "AAS/AIAA Space Flight Mechanics Meeting, Williamsburg, VA," AAS paper 15-397, 2015.

[10] Englander, J., Vavrina, M., and Hinckley, D., "Multi-objective hybrid optimal control for Multiple-flyby interplanetary mission design using Chemical propulsion," in "AIAA/AAS Astrodynamics Specialist Meeting, August 9-13 2015, Vail, CO," Paper AAS 2015-523, 2015.

[11] "The Global Trajectory Optimisation Competition Portal," http://sophia.estec.esa.int/gtoc_portal/, 2016.

[12] Sims, J. A. and Flanagan, S. N., "Preliminary Design of Low-Thrust Interplanetary Missions," in "AAS/AIAA Astrodynamics Specialist Conference," Paper AAS 99-338, Girdwood, Alaska, 1999.

[13] Gill, P. E., Murray, W., and Saunders, M. A., "SNOPT: An SQP Algorithm for Large-Scale Constrained Optimization," *SIAM J. Optim.*, Vol. 12, No. 4, 2002, pp. 979–1006, doi: 10.1137/s1052623499350013.

[14] Vinkó, T. and Izzo, D., "Global Optimisation Heuristics and Test Problems for Preliminary Spacecraft Trajectory Design," Tech. Rep. GOHTPPSTD, European Space Agency, the Advanced Concepts Team, 2008.

[15] Englander, J. A., Ellison, D. H., and Conway, B. A., "Global Optimization of Low-Thrust, Multiple-Flyby Trajectories at Medium and Medium-High Fidelity," in "AAS/AIAA Space-Flight Mechanics Meeting, Santa Fe, NM," AAS, 2014.

[16] "SPICE Ephemeris," http://naif.jpl.nasa.gov/naif/, accessed 6/26/2016.

[17] "NASA Launch Services Program Launch Vehicle Performance Web Site," http://elvperf.ksc.nasa.gov/elvMap/, accessed 6/26/2016.

[18] Pareto, V., *Manuale di Economica Politica*, Societa Editrice Libraria, Milano, Italy, 1906. Translated into English by A. Schwier as Manual of Political Economy, MacMillan Press, New York, 1971.

[19] Deb, K., Agrawal, S., Pratap, A., , and Meyarivan, T., "A fast and elitist multi-objective genetic algorithm: NSGA-II," *IEEE Transactions on Evolutionary Computation*, Vol. 6, No. 2, 2002, pp. 182–197.

[20] Holland, J. H., *Adaptation in Natural and Artificial Systems*, University of Michigan Press, 1975.

[21] Yam, C. H., Lorenzo, D. D., and Izzo, D., "Low-thrust trajectory design as a constrained global optimization problem," SAGE Publications, Vol. 225, 2011, pp. 1243–1251, doi: 10.1177/0954410011401686.

[22] Vasile, M., Minisci, E., and Locatelli, M., "Analysis of Some Global Optimization Algorithms for Space Trajectory Design," *Journal of Spacecraft and Rockets*, Vol. 47, No. 2, 2010, pp. 334–344, doi: 10.2514/1.45742.

[23] Addis, B., Cassioli, A., Locatelli, M., and Schoen, F., "A global optimization method for the design of space trajectories," *Computational Optimization and Applications*, Vol. 48, No. 3, 2009, pp. 635–652, doi: 10.1007/s10589-009-9261-6.

[24] Englander, J. A. and Englander, A. C., "Tuning Monotonic Basin Hopping: Improving the Efficiency of Stochastic Search as Applied to Low-Thrust Trajectory Optimization," in "24th International Symposium on Space Flight Dynamics, Laurel, MD," ISSFD, 2014.

[25] Peixinho, N., Doressoundiram, A., Delsanti, A., Boehnhardt, H., Barucci, M. A., and Belskaya, I., "Reopening the TNOs Color Con-

troversy: Centaurs Bimodality and TNOs Unimodality," *Astronomy and Astrophysics*, doi: 10.1051/0004-6361:20031420.

[26] Tegler, S. C., Romanishin, W., and G. J. Consolmagno, S., "Color Patterns in the Kuiper Belt: A Possible Primordial Origin," *The Astrophysical Journal Letters*, Vol. 599, No. 1, 2003, p. L49.

[27] Ortiz, J. L. et al., "Possible ring material around centaur (2060) Chiron," *Astronomy and Astrophysics*, Vol. 576, 2015, p. A18, doi: 10.1051/0004-6361/201424461.

[28] Braga-Ribas, F. et al., "A ring system detected around the Centaur (10199) Chariklo," *Nature*, Vol. 508, doi: 10.1038/nature13155.

[29] Bauer, J. M. et al., "The Large-Grained Dust Coma of 174P/Echeclus," *Publications of the Astronomical Society of the Pacific*, Vol. 120, No. 866, 2008, p. 393.

[30] "List of Centaurs and Scattered-Disk Objects," http://www.minorplanetcenter.net/iau/lists/Centaurs.html, 2016.

[31] Buie, M., Veverka, J., Johnson, L., and Adams, M., "Chiron Orbiter Mission," Tech. rep., NASA, 2010.